Intrinsic photophysics of nitrophenolate ions studied by cryogenic ion spectroscopy

Electronic Supplementary Information

Leah G. Dodson,[1,#] Wyatt Zagorec-Marks,[2,#] Shuang Xu,[3] James E. T. Smith,[2] and J. Mathias Weber[2]

[1]JILA and NIST, University of Colorado, 0440 UCB, Boulder, CO 80309-0440, USA

[2]JILA and Department of Chemistry, University of Colorado, 0440 UCB,

Boulder, CO 80309-0440, USA

[3]JILA and Department of Physics, University of Colorado, 0440 UCB,

Boulder, CO 80309-0440, USA

Table of Contents

Temperature-dependent measurements

We performed a series of experiments varying the temperature of the cold trap from 30 – 124 K, in order to measure the temperature-dependence of the *m*-nitrophenolate experimental spectrum. The figure below shows the origin region and Group 1 modes of the resulting spectra, normalized to the peak absorption of the origin 0_0^0 band at 16003 cm^{-1}. As the temperature of the ion trap is increased, the intensity of the hot bands increases relative to the 0_0^0 band intensity. In principle, one could extract the ion temperature from these measurements, assuming one knows the Franck-Condon factors and vibrational energies of the relevant bands, by measuring the change in the integrated intensities of the hot bands relative to that of the origin band.
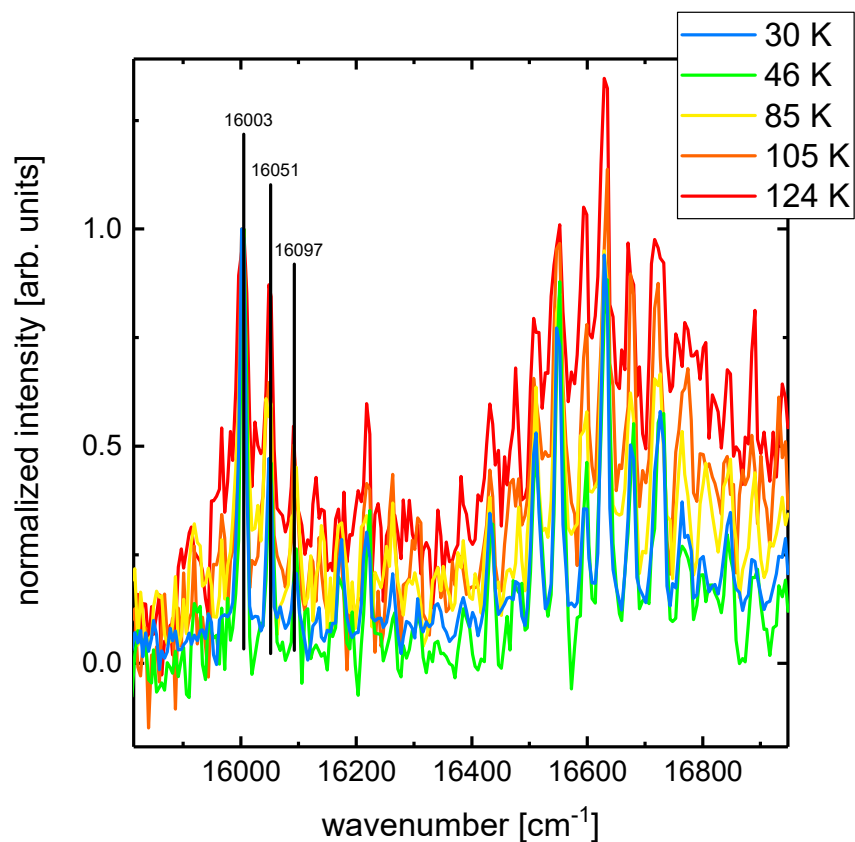
Fig. S1 Temperature-dependent *m*-nitrophenolate spectra, collected at five different trap temperatures in the electronic origin region.

The ratio of intensities of a hot band, I_1 to the origin band, I_{0-0} is equal to:

$$\frac{I_1}{I_{0-0}} = \frac{|\langle\phi_1''|\phi_1'\rangle|^2 e^{-E_1/kT}}{|\langle\phi_{0-0}''|\phi_{0-0}'\rangle|^2}$$

where $\langle\phi_1''|\phi_1'\rangle$ is the Franck-Condon overlap, E_1 is the vibrational energy of the vibrational level in the electronic ground state which gives rise to the hot band, and T is the temperature of the ion. By rearranging terms, and taking the natural logarithm of the equation, we get:

$$\ln\left(\frac{I_1}{I_{0-0}}\frac{|\langle\phi_{0-0}''|\phi_{0-0}'\rangle|^2}{|\langle\phi_1''|\phi_1'\rangle|^2}\right) = -E_1/kT.$$

We then rearrange terms again, yielding the following equation:

$$\ln\left(\frac{I_1}{I_{0-0}}\right) - \ln\left(\frac{|\langle\phi_1''|\phi_1'\rangle|^2}{|\langle\phi_{0-0}''|\phi_{0-0}'\rangle|^2}\right) = -E_1/kT.$$

Rearranging this function to obtain an equation that can be evaluated linearly gives us:

$$T = \frac{-E_1/kT}{\ln\left(\frac{I_1}{I_{0-0}}\right) - \ln\left(\frac{|\langle\phi_1''|\phi_1'\rangle|^2}{|\langle\phi_{0-0}''|\phi_{0-0}'\rangle|^2}\right)}$$

where plotting the right hand side of the previous equation versus the trap temperature should result in a straight line. Since the trap temperature does not equal the temperature of the ion, $T = T_{meas} + T_{corr}$, where T_{meas} is the temperature setting of the ion trap and T_{corr} is an additive correction term. Plotting the last equation as a function of T_{meas} produces a y-intercept value that equals T_{corr}. The values for E and ϕ are taken from the Franck-Condon simulations.

We evaluated the temperature correction term T_{corr} for the two lowest-energy hot bands, 1_1^1 and 1_2^2, at 16051 and 16097 cm^{-1}, respectively. Each data set was fit linear with a slope equal to one. For the 1_1^1 peak, $T_{corr} = (35 \pm 3)$ K, and for 1_2^2, $T_{corr} = (37 \pm 5)$ K. Therefore, data collected at a trap temperature of $T_{meas} = 30$ K are expected to represent the spectrum of ions with a temperature $T = 30 + 35$ K $= (65 \pm 5)$ K.
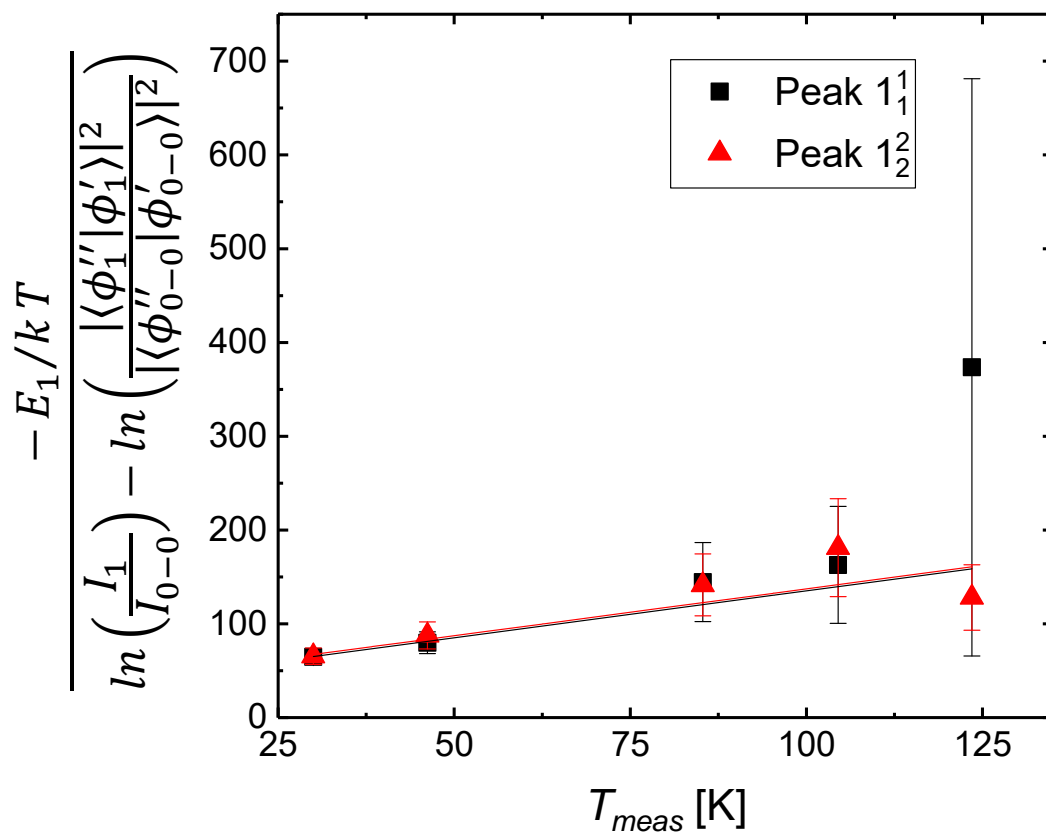
Fig. S2 Temperature dependence of the ratio of hot band intensities relative to the origin band in *m*-nitrophenolate.

Fig. S3 Frontier orbitals for *m*-, *p*-, and *o*-NP, calculated using CAM-B3LYP. Both *meta* and *para* isomers exhibit pure HOMO → LUMO transitions for $S_0 \rightarrow S_1$. The $S_0 \rightarrow S_1$ transition for *o*-NP is HOMO → LUMO+2, while the $S_0 \rightarrow S_2$ transition for *o*-NP is a mixture of HOMO−1 → LUMO+2, HOMO−1 → LUMO+6, and HOMO−3 → LUMO+2.
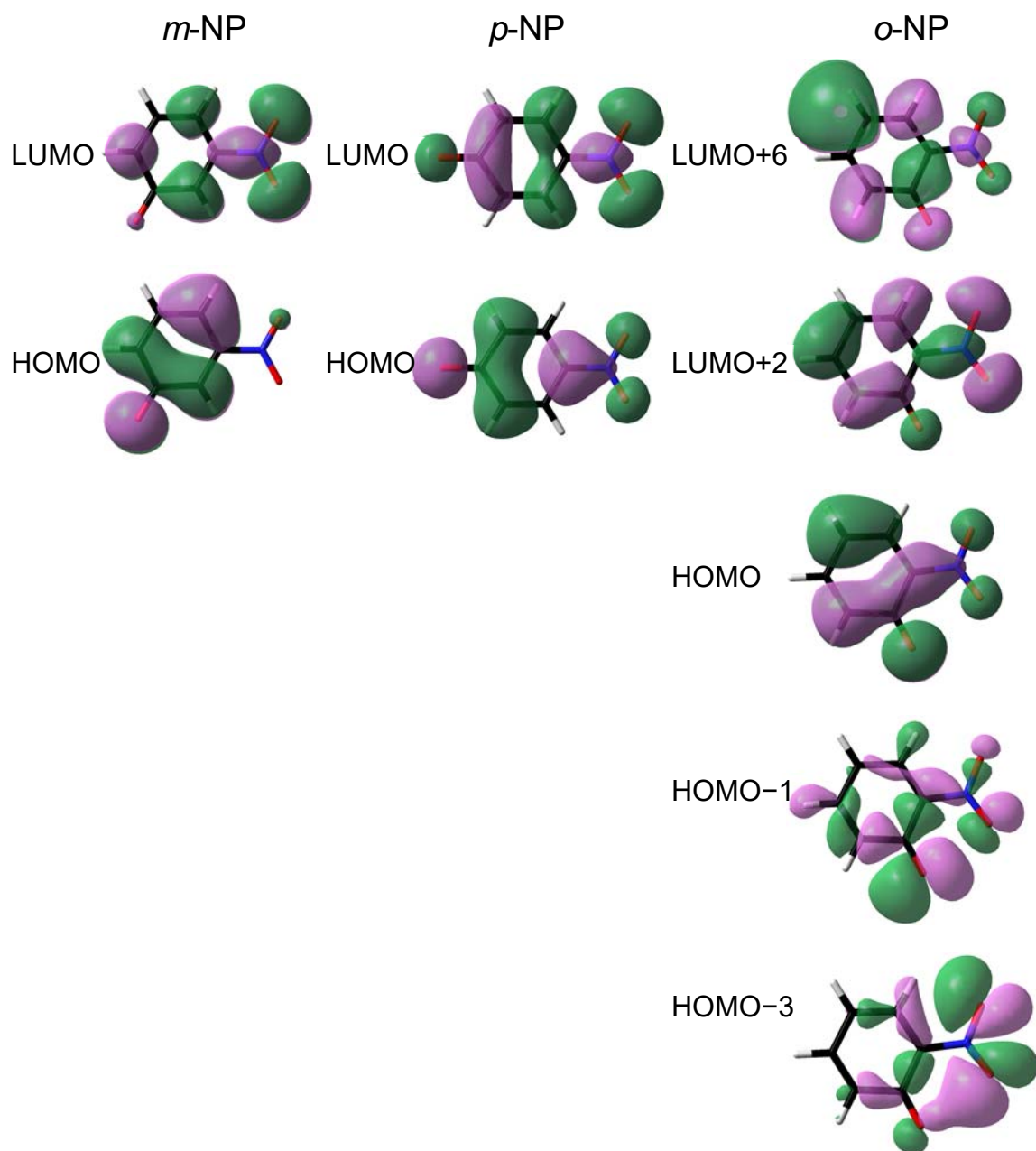
Fig. S4 Comparison of the low-temperature experimental spectra obtained in this work (in black) with the room temperature data of Brøndsted Nielsen and co-workers[1] (in red, intensity brought to the same scale).
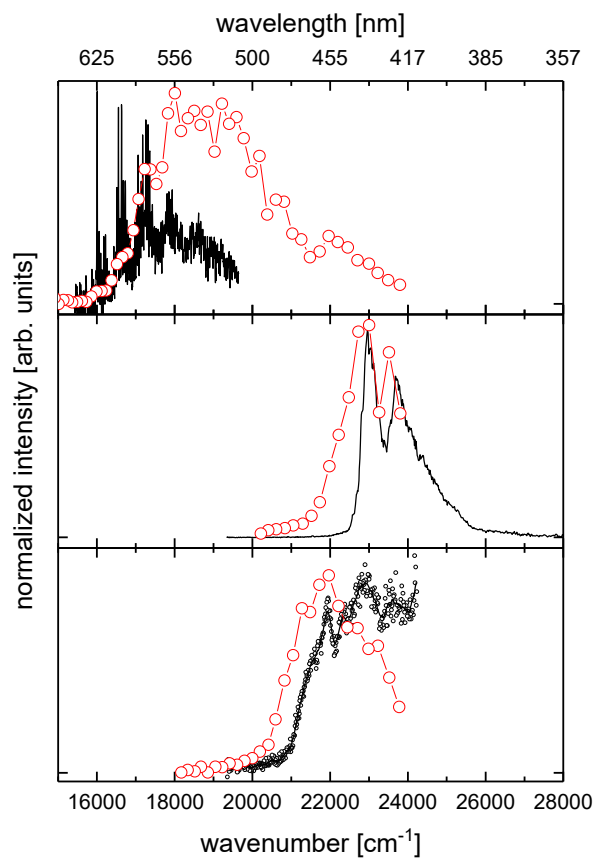
Fig. S5 Potential energy surfaces for the S_0 and S_1 states of *m*-NP. The surface was obtained at CAM-B3LYP/aug-cc-pVDZ with a relaxed scan over the nitro torsion (tors.) and pyramidalization (pyr.) coordinates. The red arrow indicates the vertical excitation from the relaxed ground state. Energies are given relative to the ground state minimum, in cm^{-1}.
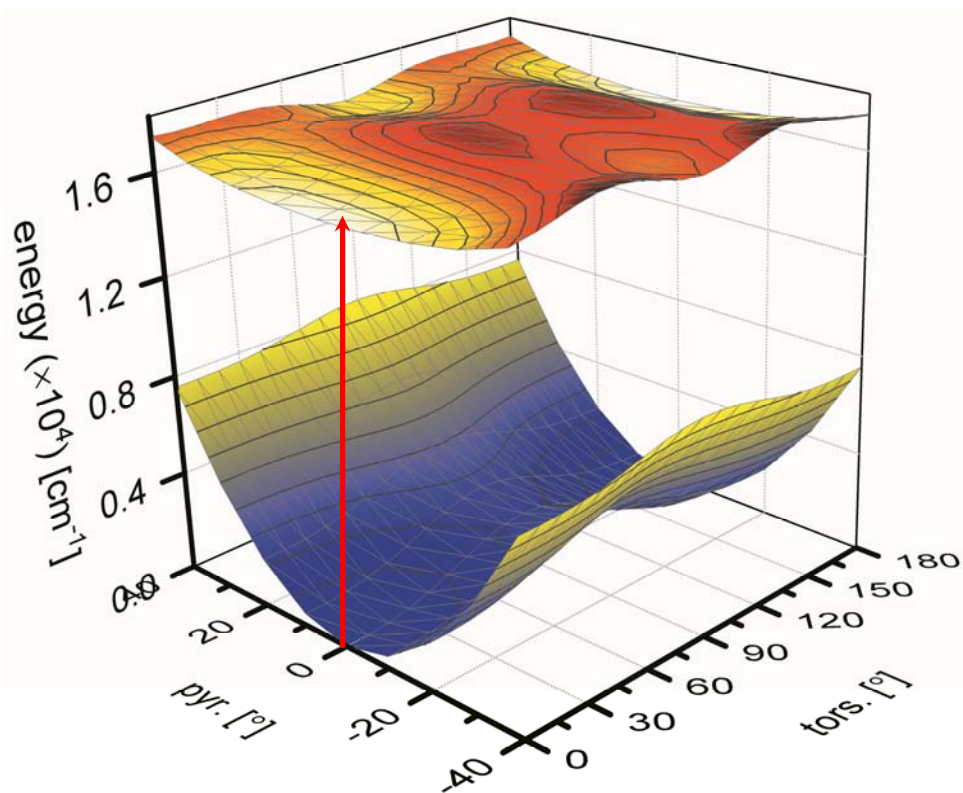
Fig. S6 One-dimension scans of *m*-NP along the torsion (tors.) coordinate of the S_0 and S_1 states using CAM-B3LYP/aug-cc-pVDZ and a NO_2 pyramidalization angle constrained to zero (corresponding to a non-pyramidalized nitro group). Energies are given relative to the minimum energy structure for each surface, in cm^{-1}.
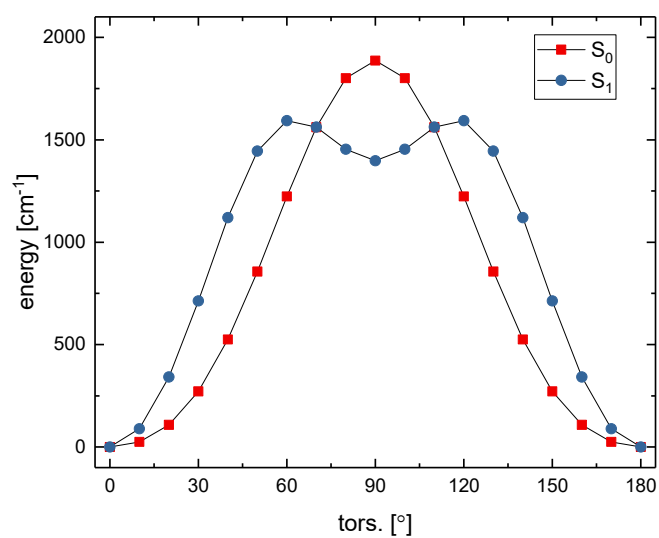
Fig. S7 Energy diagrams for the *m*-, *p*-, and *o*-nitrophenolate isomers, showing vertical energies relative to the singlet ground state minimum, in cm^{-1}. Some of the lowest-lying states are labeled, based on the point group of the ground state, i.e, without structural relaxation in the excited states.
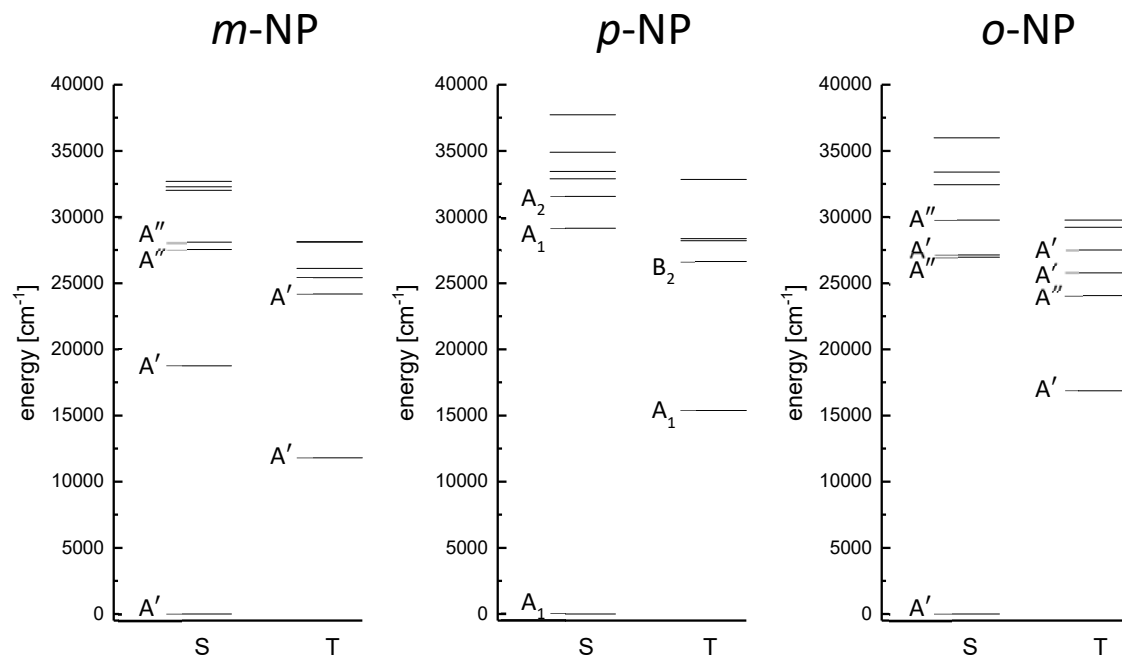
Table S1 List of calculated (CAM-B3LYP/aug-cc-pVDZ) harmonic vibrational frequencies (cm^{-1}) and symmetries for *o*-, *m*-, and *p*-NP[a]. Note that the point group is C$_s$ for *o*- and *m*-NP in both the X and A state. For *p*-NP, the X state belongs to C$_{2v}$, while the A state belongs to C$_s$.

Mode	*o*-NP X		*o*-NP A		*m*-NP X		*m*-NP A		*p*-NP X		*p*-NP A	
1	18.30	A"	41.89	A"	41.45	A"	76.95	A"	95.84	A$_2$	88.66	A"
2	107.85	A"	133.33	A"	169.14	A"	150.68	A"	103.56	B$_1$	178.59	A"
3	232.88	A"	152.85	A'	191.49	A"	213.41	A"	235.67	B$_2$	195.32	A'
4	253.02	A'	243.41	A"	228.67	A'	219.36	A'	258.73	B$_1$	257.46	A"
5	381.73	A'	337.54	A'	387.09	A'	246.72	A"	369.92	A$_1$	342.62	A'
6	429.30	A'	385.02	A"	439.62	A'	384.46	A'	439.32	A$_2$	373.87	A"
7	438.88	A"	456.38	A'	452.86	A"	439.41	A'	451.21	B$_2$	449.46	A'
8	546.34	A"	533.96	A"	526.84	A'	443.86	A"	487.26	B$_1$	526.02	A"
9	565.75	A'	551.90	A'	563.49	A'	524.99	A'	551.72	B$_2$	546.87	A'
10	572.62	A'	636.22	A'	571.67	A"	563.57	A'	635.38	B$_2$	586.49	A'
11	662.60	A'	642.78	A"	683.07	A'	578.51	A"	648.04	A$_1$	638.26	A'
12	723.45	A"	673.86	A'	693.17	A"	654.18	A'	731.44	B$_1$	684.33	A"
13	750.86	A"	761.27	A"	730.67	A"	690.02	A"	801.08	B$_1$	772.77	A'
14	810.20	A"	783.74	A"	804.41	A"	760.99	A'	801.17	A$_2$	785.47	A"
15	825.06	A'	804.02	A'	843.22	A'	792.14	A"	822.78	A$_1$	830.39	A'
16	870.95	A"	857.18	A'	876.43	A"	880.08	A"	859.05	A$_1$	891.18	A"
17	893.67	A'	873.30	A"	902.22	A"	920.26	A'	883.99	B$_1$	983.00	A"
18	989.44	A"	959.42	A"	941.83	A'	944.17	A"	994.96	A$_1$	994.74	A'
19	998.41	A"	988.95	A"	982.56	A"	992.64	A"	1002.07	B$_1$	1005.41	A"
20	1037.80	A'	1075.13	A'	999.61	A'	996.77	A'	1002.50	A$_2$	1106.33	A'
21	1088.28	A'	1098.15	A'	1086.55	A'	1067.83	A'	1104.90	B$_2$	1121.61	A'
22	1146.37	A'	1163.38	A'	1094.06	A'	1077.58	A'	1138.07	A$_1$	1174.08	A'
23	1169.23	A'	1169.50	A'	1159.89	A'	1149.67	A'	1204.68	A$_1$	1248.25	A"
24	1241.75	A'	1260.46	A'	1256.62	A'	1240.35	A'	1271.77	B$_2$	1276.04	A'
25	1306.43	A'	1287.42	A'	1314.93	A'	1307.92	A'	1333.94	B$_2$	1318.99	A'
26	1379.71	A'	1344.05	A"	1400.13	A'	1374.15	A'	1371.93	A$_1$	1349.64	A"
27	1407.01	A'	1360.85	A'	1425.16	A'	1424.24	A'	1429.24	A$_1$	1387.72	A'
28	1495.56	A'	1389.56	A'	1498.42	A'	1454.57	A'	1501.01	B$_2$	1490.38	A'
29	1540.07	A'	1440.25	A'	1572.31	A'	1489.5	A'	1544.21	B$_2$	1500.70	A'
30	1581.74	A'	1559.89	A'	1578.25	A'	1524.57	A'	1591.06	B$_2$	1548.00	A'
31	1639.01	A'	1651.33	A'	1616.85	A'	1613.77	A'	1619.21	A$_1$	1628.51	A'
32	1691.94	A'	1693.12	A'	1669.72	A'	1647.13	A'	1674.01	A$_1$	1680.80	A'
33	3152.44	A'	3180.48	A'	3158.84	A'	3179.16	A'	3191.61	B$_2$	3204.36	A'
34	3194.28	A'	3201.21	A'	3189.66	A'	3217.54	A'	3192.30	A$_1$	3204.91	A'
35	3200.83	A'	3219.28	A'	3248.6	A'	3261.33	A'	3228.38	B$_2$	3224.74	A'

Table S2 Assignment of transitions in the origin region of *m*-NP[a]

Observed transition (cm^{-1})	Assignment	Calculated transition (cm^{-1})[b]	Intensity
15910	1^0_2	15766	1226
15963	1^1_3	15812	1574
16003	0^0_0	15849	118900
16051	1^1_1	15895	50890
16097	1^2_2	15940	19670
16133	1^3_3	15986	6754
16175	1^2_0	16023	5178
16221	1^3_1	16068	6646
16263	1^4_2	16114	5409
16308	1^5_3	16159	3475

[a] Calculations performed at CAM-B3LYP/aug-cc-pVDZ

[b] Excited state mode 1 vibrational frequency has been scaled by 1.13

Table S3 Assignment of group 1 transitions in *m*-NP[a]

Observed transition (cm^{-1})	Assignment	Calculated transition (cm^{-1})[b]	Intensity
16435	7_0^1	16288	33080
16479	$1_1^1 7_0^1$	16334	14150
16513	9_0^1	16374	26470
16551	10_0^1	16413	74150
	$1_1^1 9_0^1$	16419	11330
16597	$1_2^2 9_0^1$	16465	4378
	$1_1^1 10_0^1$	16458	31720
16632	$1_2^2 10_0^1$	16504	12260
	12_0^1	16503	84000
16679	$1_1^1 12_0^1$	16549	35940
	$1_3^3 10_0^1$	16549	4210
16726	$1_2^2 12_0^1$	16594	13890
16766	14_0^1	16610	38520
16802	$1_1^3 10_0^1$	16632	4141
	$1_3^3 12_0^1$	16640	4769
16824	$1_1^1 14_0^1$	16655	16480
16847	$1_2^2 14_0^1$	16701	6370
16876	$1_1^3 12_0^1$	16723	4691
16886	7_0^2	16728	4656

[a] Calculations performed at CAM-B3LYP/aug-cc-pVDZ

[b] Excited state mode 1 vibrational frequency has been scaled by 1.13

Table S4 Assignment of group 2 transitions in *m*-NP[a]

Observed transition (cm^{-1})	Assignment	Calculated transition (cm^{-1})[b]	Intensity
16931	$7_0^1 9_0^1$	16813	6915
16976	$7_0^1 10_0^1$	16852	19990
17021	$1_1^1 7_0^1 10_0^1$	16897	8552
17061	21_0^1	16917	5478
	22_0^1	16927	9464
	$9_0^1 10_0^1$	16938	17320
	$7_0^1 12_0^1$	16943	23130
17095	$1_1^1 22_0^1$	16972	4049
	10_0^2	16976	23210
17108	$1_1^1 9_0^1 10_0^1$	16983	7408
	$1_3^3 7_0^1 10_0^1$	16988	9894
17140	$1_1^1 10_0^2$	17022	9929
	$9_0^1 12_0^1$	17028	18950
17178	$7_0^1 14_0^1$	17049	10720
	$10_0^1 12_0^1$	17067	50450
17190	$1_1^1 9_0^1 12_0^1$	17074	8108
17219	$1_1^1 7_0^1 14_0^1$	17095	4587
	$1_1^1 10_0^1 12_0^1$	17112	21580
17233	$9_0^1 14_0^1$	17135	8602
17261	12_0^2	17157	26230
	$1_2^2 10_0^1 12_0^1$	17158	8341
17275	$10_0^1 14_0^1$	17174	24060
17299	$1_1^1 12_0^2$	17203	11220
17312	$1_1^1 10_0^1 14_0^1$	17219	10290
	26_0^1	17223	33340
17356	$12_0^1 14_0^1$	17264	22610
	$1_1^1 26_0^1$	17269	14260

17377	27_0^1	17273	20070
17387	28_0^1	17304	19510
	$1_1^1 12_0^1 14_0^1$	17310	9674
17397	$1_2^2 26_0^1$	17314	5512
	$1_1^1 27_0^1$	17319	8585
17427	$1_1^1 28_0^1$	17349	8345
17446	unassigned		
17475	14_0^2	17371	4743
	30_0^1	17374	4026
17489	$7_0^1 9_0^1 10_0^1$	17377	4391
17520	$7_0^1 10_0^2$	17416	6066
17569	31_0^1	17463	15050
	$7_0^1 9_0^1 12_0^1$	17468	4903
17593	$10_0^1 22_0^1$	17490	6117
17604	$9_0^1 10_0^2$	17501	5680
	$7_0^1 10_0^1 12_0^1$	17506	13460
	$1_1^1 31_0^1$	17508	6437
17639	10_0^3	17540	4865
17651	$1_1^1 7_0^1 10_0^1 12_0^1$	17552	5756
17685	$12_0^1 22_0^1$	17581	5911
	$9_0^1 10_0^1 12_0^1$	17592	11960
17697	$7_0^1 12_0^2$	17597	7144
17735	$7_0^1 10_0^1 14_0^1$	17613	6493
	$10_0^2 12_0^1$	17630	15210
	$1_1^1 9_0^1 10_0^1 12_0^1$	17637	5114

[a] Calculations performed at CAM-B3LYP/aug-cc-pVDZ

[b] Excited state mode 1 vibrational frequency has been scaled by 1.13

Table S5 Assignment of group 3 transitions in *m*-NP[a]

Observed transition (cm^{-1})	Assignment	Calculated transition (cm^{-1})[b]	Intensity
17759	$7_0^1 26_0^1$	17663	9061
	$1_1^1 10_0^2 12_0^1$	17676	6507
17768	$9_0^1 12_0^2$	17682	6012
17785	$9_0^1 10_0^1 14_0^1$	17699	5637
	$7_0^1 12_0^1 14_0^1$	17704	6227
17802	$7_0^1 27_0^1$	17713	5070
	$10_0^1 12_0^2$	17721	15100
17850	$10_0^2 14_0^1$	17737	7546
17865	$7_0^1 28_0^1$	17743	4755
	$9_0^1 26_0^1$	17748	7546
17896	$1_1^1 10_0^1 12_0^2$	17766	6461
	$10_0^1 26_0^1$	17787	20800
	$9_0^1 12_0^1 14_0^1$	17789	5129
17919	$9_0^1 27_0^1$	17798	4651
	12_0^3	17812	4716
	$10_0^1 12_0^1 14_0^1$	17828	13570
17936	$9_0^1 28_0^1$	17829	4179
	$1_1^1 10_0^1 26_0^1$	17832	8897
	$10_0^1 27_0^1$	17837	12780
17971	$10_0^1 28_0^1$	17867	12470
	$1_1^1 10_0^1 12_0^1 14_0^1$	17873	5804
17981	$12_0^1 26_0^1$	17877	23660
	$1_1^1 10_0^1 27_0^1$	17882	5465
18017	$1_1^1 10_0^1 28_0^1$	17913	5334
	$12_0^2 14_0^1$	17918	5613
	$1_1^1 12_0^1 26_0^1$	17923	10120
18025	$12_0^1 27_0^1$	17927	14520

18053	$12_0^1 28_0^1$	17958	13560
18069	$1_1^1 12_0^1 27_0^1$	17973	6213
	$14_0^1 26_0^1$	17984	9808
18088	$1_1^1 12_0^1 28_0^1$	18003	5798
18139	$10_0^1 31_0^1$	18026	9401
	$1_1^1 14_0^1 26_0^1$	18030	4195
18153	$14_0^1 27_0^1$	18034	6358
18196	$14_0^1 28_0^1$	18065	5716
18221	$12_0^1 31_0^1$	18117	11700
18265	$1_1^1 12_0^1 31_0^1$	18162	5004

[a] Calculations performed at CAM-B3LYP/aug-cc-pVDZ

[b] Excited state mode 1 vibrational frequency has been scaled by 1.13

References

1. M. Wanko, J. Houmoller, K. Stochkel, M.-B. S. Kirketerp, M. Å. Petersen, M. Brøndsted Nielsen, S. Brøndsted Nielsen and A. Rubio, *Phys. Chem. Chem. Phys.*, 2012, **14**, 12905-12911.